N-cadherin prevents the premature differentiation of anterior heart field progenitors in the pharyngeal mesodermal microenvironment

Open
ORIGINAL ARTICLE

Cell Research (2014) 24:1420-1432.

www.nature.com/cr

N-cadherin prevents the premature differentiation of anterior heart field progenitors in the pharyngeal mesodermal microenvironment

Boon-Seng Soh[1, 2, 3, 4, *], Kristina Buac[1, 2, 5, *], Huansheng Xu[1, 2, 3, *], Edward Li[1], Shi-Yan Ng[2], Hao Wu[1, 2], Jolanta Chmielowiec[1, 2], Xin Jiang[1, 2], Lei Bu[1, 2, 3], Ronald A Li[3, 6], Chad Cowan[1, 2], Kenneth R Chien[1, 2, 4]

[1]Cardiovascular Research Center, Massachusetts General Hospital, 185 Cambridge Street, Boston, MA 02114, USA; [2]Department of Stem Cell and Regenerative Biology, Harvard University and Harvard Medical School, 7 Divinity Avenue, Cambridge, MA 02138, USA; [3]Stem Cell & Regenerative Medicine Consortium, and the Department of Physiology, LKS Faculty of Medicine, The University of Hong Kong, Hong Kong SAR, China; [4]Department of Cell and Molecular Biology and Medicine, Karolinska Institute, 171 77 Stockholm, Sweden; [5]Department of Biochemistry and Molecular Biology, University of Georgia, Athens, GA 30602, USA; [6]Center of Cardiovascular Research, Mount Sinai School of Medicine, New York, NY 10029, USA

The cardiac progenitor cells (CPCs) in the anterior heart field (AHF) are located in the pharyngeal mesoderm (PM), where they expand, migrate and eventually differentiate into major cell types found in the heart, including cardiomyocytes. The mechanisms by which these progenitors are able to expand within the PM microenvironment without premature differentiation remain largely unknown. Through *in silico* data mining, genetic loss-of-function studies, and *in vivo* genetic rescue studies, we identified N-cadherin and interaction with canonical Wnt signals as a critical component of the microenvironment that facilitates the expansion of AHF-CPCs in the PM. CPCs in N-cadherin mutant embryos were observed to be less proliferative and undergo premature differentiation in the PM. Notably, the phenotype of N-cadherin deficiency could be partially rescued by activating Wnt signaling, suggesting a delicate functional interaction between the adhesion role of N-cadherin and Wnt signaling in the early PM microenvironment. This study suggests a new mechanism for the early renewal of AHF progenitors where N-cadherin provides additional adhesion for progenitor cells in the PM, thereby allowing Wnt paracrine signals to expand the cells without premature differentiation.

***Keywords*:** N-cadherin; anterior heart field; cardiac progenitor cells; premature differentiation; Wnt signaling; microenvironment

Cell Research (2014) **24**:1420-1432. doi:10.1038/cr.2014.142; published online 4 November 2014

Introduction

The mammalian heart arises from two regions of the multipotent cells in the splanchnic mesoderm, previously described as the first heart field (FHF) and second heart field (SHF). While the FHF progenitors give rise to the left ventricle and the inflow tract (IFT), cells from the SHF (Isl1+) contribute to the development of the right ventricle, outflow tract (OFT) and parts of the IFT [1-3].

The anterior heart field (AHF)-cardiac progenitor cells (CPCs), identified as a subset of the SHF marked by expression of Mef2c marker [1], reside within the pharyngeal mesoderm (PM) during early cardiogenesis and receive inputs from a variety of surrounding cell types through signaling pathways such as Bmp [4], Fgf [5-7], Shh [8], Notch [9] and Wnt [10-12], to direct their self-renewal, migration and differentiation. Although the PM serves as the niche for AHF cardiac progenitors before they migrate and differentiate into cardiac structures such as the OFT and RV, the establishment and regulation of this microenvironment remains largely unknown. At present, many established models of stem/progenitor

*These three authors contributed equally to this work.
Correspondence: Kenneth R Chien
E-mail: kenneth.chien@ki.se
Received 22 March 2014; revised 4 July 2014; accepted 23 September 2014; publsihed online 4 November 2014

cell niche have reported the requirement for cell adhesion proteins in niche establishment and cell regulation [13-15]. These reports prompted us to investigate the function of cell adhesion proteins in the microenvironment of AHF progenitors during early cardiogenesis.

Cadherins are calcium-dependent adhesion molecules that play an important role in cell adhesion by forming adherens junctions that bind cells within tissues together. Previous work by Linask *et al*. [16] have shown that in the avian embryo after mesodermal separation into somatic and splanchnic (precardiac) mesoderm, ubiquitous N-cadherin, a prominent member of the calcium-dependent cell adhesion protein family, expression becomes restricted to the precardiac mesoderm, and it is specifically localized to the apical surface of the precardial cells. The N-cadherin expression co-localized with β-catenin at this stage [17]. During further stages of development, N-cadherin becomes evenly incorporated into the adherent junctions of the differentiated cardiomyocytes in the tubular myocardium. Subsequently, inhibition of N-cadherin signaling with N-cadherin blocking antibody leads to severe perturbation in heart formation depending on the timing and duration of the inhibition [17]. Further studies in mice have shown that N-cadherin is expressed in cardiac tissues during early developmental stages: E7.5 in the cardiac crescent, E8.5 in the linear heart tube, E9.5 in the looped heart, and continues to be expressed in the adult myocardium [18]. Because N-cadherin is highly expressed throughout the adult myocardium, its deletion at this stage leads to arrhythmogenesis due to the disassembly of gap junctions required for intercellular ion flow and cardiac action potential propagation [19]. Collectively, the expression pattern of N-cadherin and functional studies indicate that this cell adhesion molecule plays a critical role in the heart organogenesis.

In this study, through *in silico* data mining and genetic loss-of-function approaches, we demonstrated that N-cadherin is required for the establishment and maintenance of AHF-CPCs. Loss of N-cadherin results in diminished proliferation of the CPCs in the PM, as well as their premature differentiation into Tnt+ cells. Importantly, the cardiac phenotype exhibited by N-cadherin mutants can be partially rescued by overexpression of Wnt signaling.

Results

CPCs express N-cadherin in the PM

The AHF progenitors reside within the PM before they migrate to the elongating heart tube. In an attempt to identify the components of the microenvironment of the Isl1+ CPCs in the AHF, we analyzed microarray data containing the transcriptional profiles of CPCs derived from mouse ES cells. The generation of the microarray dataset has been previously described [20]. Focusing on genes categorized under the gene ontology term "cell-cell adhesion" (GO: 160037), and comparing their expressions in the Isl1+ CPCs to those in non-cardiac cells, *Cdh2* was found to be among the top genes that were significantly enriched in the CPCs (Figure 1A and 1B). The gene *Cdh2* encodes for N-cadherin, a Ca^{2+}-dependent adhesion molecule. N-cadherin has been implicated in epithelial-mesenchymal transition (EMT), a process involved in many developmental and pathological events, including the formation of splanchnic mesoderm from primitive streaks [21].

Indeed, previous studies have reported the importance of cadherins in progenitor/stem cell niche establishment and regulation. Examination of both cadherins (E-cad and N-cad) in E9.5 embryos revealed that E-cadherin is only expressed in the pharyngeal endoderm and the surrounding epithelial structures, while N-cadherin is detected in the PM and heart tube (Figure 1C and 1D; yellow arrows). Furthermore, analysis of *Mef2c* expression

Figure 1 N-cadherin expression in embryonic stem cell-derived AHF cardiac progenitors. **(A)** "Cell-cell adhesion" genes enriched in embryonic stem cell-derived cardiac progenitor cells identified through the analysis of the microarray dataset reported by Domian *et al.* [20]. **(B)** Quantitative PCR analysis of N-cadherin expression (Cdh2) in cardiac progenitor cells (CPCs) derived from day 6 embryoid bodies (EBs) compared to non-cardiac cells (control) isolated from the same EBs. Error bars indicate SD, $n = 3$ experiments, $^*P < 0.05$, evaluated by Student's *t*-test. **(C)** Representative sagittal section of wild-type mouse embryo (E9.5) immunostained for E-cadherin (red). Enlarged image shows a lack of E-cadherin expression in the PM (indicated by white arrows). Nuclei were marked by DAPI. Scale bar, 200 μm. **(D)** Sagittal section of wild-type mouse embryo (E9.5) immunostained for N-cadherin (red) and Mef2c (green). N-cadherin expression increases anteriorly towards the outflow tract (OFT) (yellow arrows). Coincident with the increase in N-cadherin expression was an increase in Mef2c expression, an important myocardial cell differentiation marker. Nuclei were marked by DAPI. Scale bar, 200 μm. **(E)** Immunofluorescence on sagittal section of wild-type mouse embryo at E9.0. N-cadherin (red) is weakly expressed in the Isl1+ (green) CDCs in the AHF (enlarged image). Arrows indicate strong N-cadherin expression in differentiated cardiomyocytes within the heart tube. Section orientation is as shown: A, anterior; P, posterior; D, Dorsal; V, ventral. Scale bar, 20 μm. **(F)** N-cadherin expression in CPCs compared to cardiomyocytes (CMs). The analysis was based on microarray datasets reported by Domian *et al.* [20].

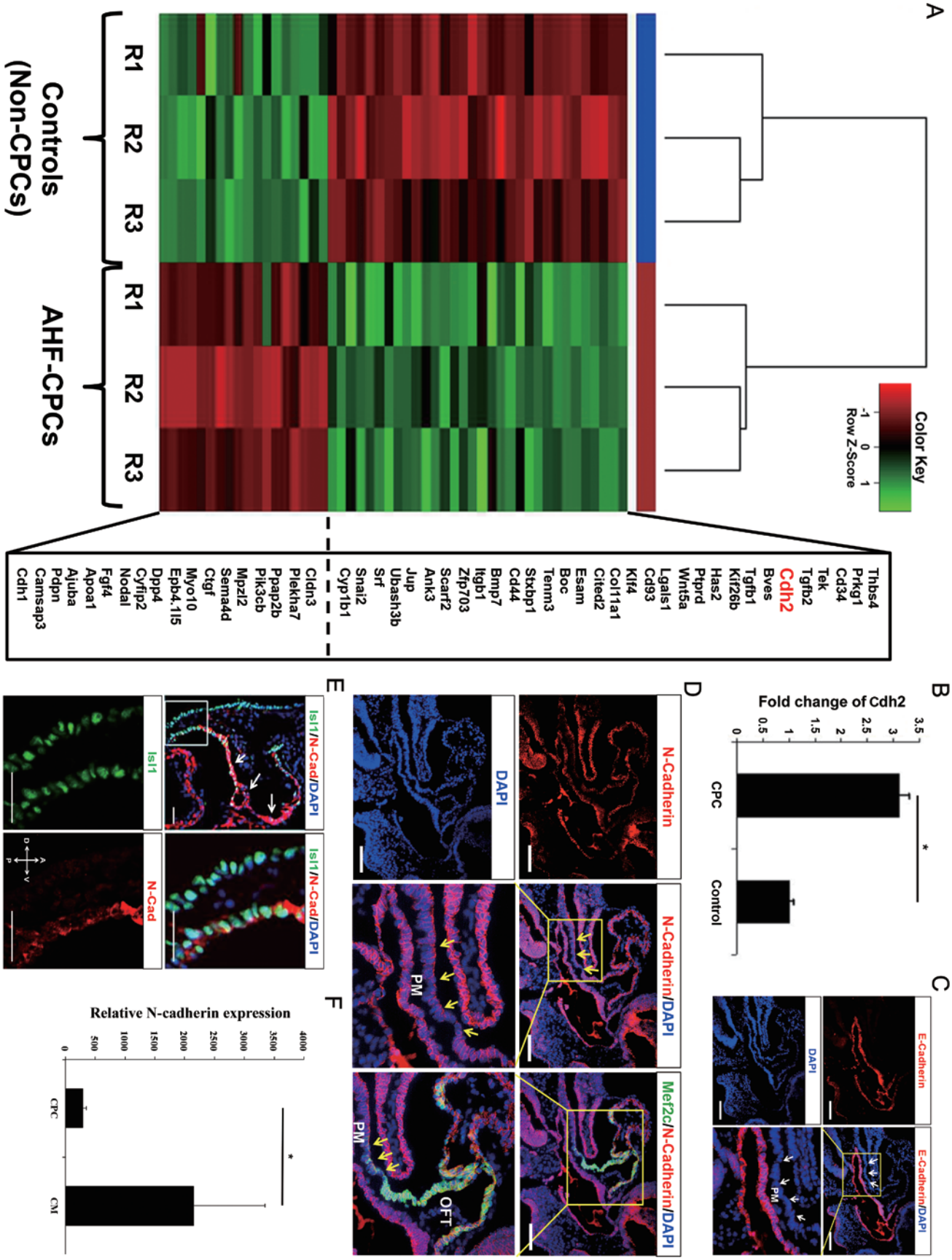
A
Color Key
Row Z-Score
-1
0
1
R1
R2
R3
R1
R2
R3
Controls (Non-CPCs)
AHF-CPCs
Thbs4
Prkg1
Cd34
Tek
Tgfb2
Cdh2
Bves
Tgfb1
Kif26b
Has2
Ptprd
Wnt5a
Lgals1
Cd93
Klf4
Col11a1
Cited2
Esam
Boc
Tenm3
Stxbp1
Cd44
Bmp7
Itgb1
Zfp703
Scarf2
Ank3
Jup
Ubash3b
Srf
Snai2
Cyp1b1
Cldn3
Plekha7
Ppap2b
Pik3cb
Mpzl2
Sema4d
Ctgf
Myo10
Epb4.1l5
Dpp4
Cyfip2
Nodal
Fgf4
Apoa1
Ajuba
Pdpn
Camsap3
Cdh1
B
Fold change of Cdh2
3.5
3
2.5
2
1.5
1
0.5
0
CPC
Control
*
C
E-Cadherin
E-Cadherin/DAPI
DAPI
PM
D
N-Cadherin
N-Cadherin/DAPI
Mef2c/N-Cadherin/DAPI
DAPI
PM
OFT
E
Isl1/N-Cad/DAPI
Isl1
N-Cad
D
V
A
P
F
Relative N-cadherin expression
4000
3500
3000
2500
2000
1500
1000
500
0
CPC
CM
*

in the developing embryo at E9.5 revealed co-expression with N-cadherin (Figure 1D). These results indicate that E-cadherin is not expressed in AHF progenitors and thus is likely not required for the establishment of the progenitor microenvironment in the PM and regulation of the progenitor activity.

Next, to study the potential function of Cdh2 in Isl1+ CPCs, we examined the expression of N-cadherin in AHF-CPCs. Consistent with earlier results, immunostaining on sagittal sections of wild-type embryos at embryonic day E9.0 demonstrated weak expression of N-cadherin in the CPCs (Isl1+) within the AHF (Figure 1E). Interestingly, N-cadherin expression was higher in the OFT and heart tube when compared to PM (Figure 1E and 1F). Coincident with the increase in N-cadherin expression was an increase in Mef2c expression (Figure 1D).

From these results, it is clear that the expression of N-cadherin not only overlaps with Isl1 expression in the PM but its expression level also increases, alongside with Mef2c, as the AHF-CPCs migrate out of PM to form the OFT and ventricles. This suggests that N-cadherin possibly plays a role in the maintenance of the CPC microenvironment in the PM.

Deletion of N-cadherin in AHF cardiac progenitors resulted in decreased progenitor cell population size and hypoplastic cardiac OFT and right ventricle

To study the function of N-cadherin in Isl1+ CPCs, we performed conditional gene knockout using the Cre-loxP system. Because the Cre is expressed under the control of AHF-specific enhancer, its expression is restricted to the CPCs and their progenies [22]. In N-cadherin conditional mutant mouse line, the first exon containing the start codon is flanked by loxP sites [23], resulting in a Cdh2 floxed allele (*Cdh2*^{fl}). To delete N-cadherin specifically in AHF-CPCs, we crossed double-heterozygous (*AHF-Cre*; *Cdh2*$^{fl/+}$) male mice with females homozygous for the *Cdh2*^{fl} allele (*Cdh2*$^{fl/fl}$). The disruption of N-cadherin expression in the AHF-CPCs caused embryonic lethality around E9.5-E10.5, with no viable embryos retrieved at E11.5 (Figure 2A). Examination of the mutant embryos at E9.0-E9.5 revealed that all of them contained defects in the cardiac OFT and right ventricle. The cardiac OFT in the mutants was found to be shorter compared to that in the control embryos (Figure 2B and 2C). The looping of the developing heart is also abnormal, with the mutant cardiac OFT and RV protruding forward instead of turning toward the body (Figure 2B and 2C). This phenotype suggests disrupted growth of the cardiac OFT and RV. The disruption in growth could be attributed to defects in CPCs that contribute to the OFT and RV.

To address this, we examined the CPC population at this stage of the embryo. Utilizing a transgenic mouse line where GFP is expressed under the AHF-specific enhancer [12], labeling of CPCs was achieved with GFP. Visual inspection indicated that the GFP+ progenitor cell population in the AHF region decreased in the N-cadherin mutants as compared to that in control embryos (Figure 2C). Employing flow cytometry to quantitate the number of GFP+ cells in the AHF region only (not including the OFT and RV), we found that the number of CPCs decreased by over 60% in the mutants (Figure 2D). Consistently, a similar decrease was observed in N-cadherin-deficient progenitor cells in day 6 embryoid bodies derived from transgenic *AHF-Cre*; *AHF-GFP*; *Cdh2*$^{fl/fl}$ mES cells (Figure 2E and 2F). These results indicate that loss of N-cadherin leads to a decreased number of CPCs, which could contribute to the hypoplastic cardiac OFT and RV phenotypes in the mutant embryos.

Deletion of N-cadherin resulted in decreased proliferation and premature differentiation of Isl1+ cardiac progenitors

We reasoned that the decreased number of CPCs could be due to disrupted proliferation or augmented apoptosis as a result of N-cadherin deletion. To test this, immunostaining for phosphorylated histone 3 (PiH3), a mitotic marker, was performed to assess the proliferation of the Isl1+ CPCs in E9.5 embryos. We found that the mitotic index of the CPCs (Isl1 and PiH3 dual-positive cells) in the mutant embryos (*AHF-Cre*; *Cdh2*$^{fl/fl}$) was significantly lower than that in the control embryos, although the mitotic index in the neuroepithelial cells of brain remained the same for both the wild-type and mutant embryos (Figure 3A and 3B), indicating that the decrease in proliferation was specific to the Isl+ cells within AHF.

To investigate whether deletion of N-cadherin results in an increased apoptosis of the CPCs, we performed immunostaining for Isl1 and cleaved Caspase 3. We also assessed the level of apoptosis in differentiated cardiomyocytes by performing immunostaining for cardiac troponin T (cTnT) and cleaved Caspase 3 (Supplementary information, Figure S1). The results further revealed that despite the increase in number of cells undergoing apoptosis in mutant embryos, the majority of apoptotic cells are present outside of the PM, OFT and RV (Figure 3C). A small number of apoptotic cells, however, were found to be present at the venous pole of the heart, which is also contributed by the AHF-Cre line (Supplementary information, Figure S1). This result is consistent with previous studies, which showed that cell-cell contact mediated by N-cadherin is important for smooth muscle cell proliferation and survival [24, 25]. Taken together, these

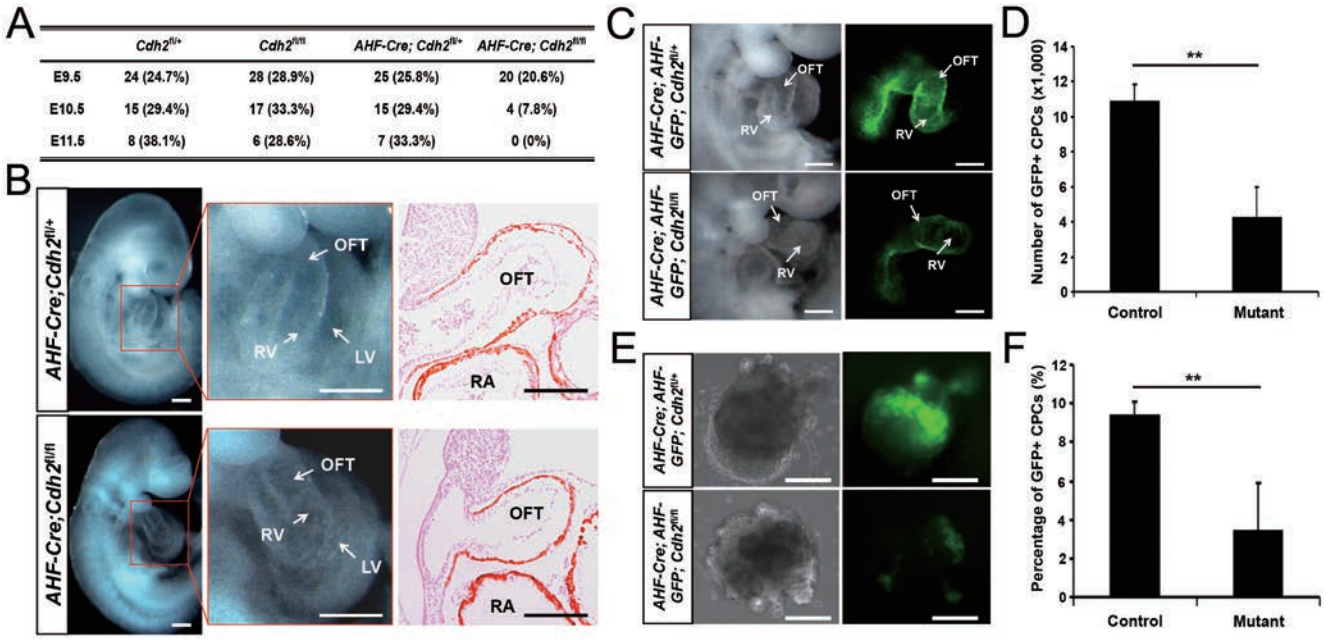

	$Cdh2^{fl/+}$	$Cdh2^{fl/fl}$	AHF-Cre; $Cdh2^{fl/+}$	AHF-Cre; $Cdh2^{fl/fl}$
E9.5	24 (24.7%)	28 (28.9%)	25 (25.8%)	20 (20.6%)
E10.5	15 (29.4%)	17 (33.3%)	15 (29.4%)	4 (7.8%)
E11.5	8 (38.1%)	6 (28.6%)	7 (33.3%)	0 (0%)

Figure 2 Impaired development of AHF derivatives in AHF-specific Cdh2 mutant. **(A)** The percentage of surviving embryos dissected at various embryonic stages compared to expected Mendelian ratio. Note that mutant embryos are dying between E10.5 and E11.5. Viability was measured by the presence of a heartbeat. **(B)** AHF-specific Cdh2 mutant embryos exhibit hypoplastic cardiac outflow tract (OFT) compared to controls at E9.5. H&E staining of the sagittal sections revealed smaller OFT in the mutant at E9.5 (enlarged image). Cardiomyocytes are stained dark red. Scale bar, 200 μm. **(C)** Whole embryo images of AHF-GFP expression in control and mutant embryos. Note reduction in the GFP expression in the mutants as well as shortened OFT and hypoplastic RV. Scale bar, 200 μm. **(D)** GFP sorted cells isolated from control and mutant embryos. Cdh2 mutants show reduced number of AHF-GFP+ cells (~60%) compared to the wild-type control. Error bars indicate SD, $n = 4$ experiments, $^{**}P = 0.003$, evaluated by Student's *t*-test. **(E)** Representative image of day 6 embryoid bodies (EB) differentiated from transgenic *AHF-Cre*$^{+/-}$; *AHF-GFP*$^{+}$; *Cdh2*$^{fl/+}$ (top panel) and *AHF-Cre*$^{+/-}$; *AHF-GFP*$^{+}$; *Cdh2*$^{fl/fl}$ (bottom panel) ES cells. Note the reduction in GFP expression in the mutant EBs. Scale bar, 200 μm. **(F)** Quantification of GFP+ cells isolated from control and mutant EBs. Error bars indicate SD, $n = 3$ experiments, $^{**}P = 0.01$, evaluated by Student's *t*-test.

results suggest that the increase in apoptosis observed in the areas outside the heart in the conditional *cdh2* mutant compared to wild type is mostly a secondary effect of embryo death, presumably due to inadequate supply of oxygen and nutrients to the rest of the body.

Interestingly, we observed ectopic cTnT-expressing cells in the AHF region of the mutant embryos (Figure 3D and 3E). Cardiac troponin T, a marker of differentiated cardiomyocytes, is not commonly found in the AHF region. The increased number of cTnT+ cells in the AHF of the mutants suggests that loss of N-cadherin signaling within AHF leads to premature differentiation of Isl1+ CPCs. Taken together, the results suggest that N-cadherin plays an important role in the maintenance of the AHF-CPC microenvironment to enhance progenitor cell proliferation and prevent premature differentiation.

Stabilization of β-catenin molecules partially rescued the Cdh2 mutant phenotype

Previously, it was demonstrated that the Wnt/β-catenin signaling pathway plays an important role in the development of Isl1+ CPCs. Specifically, enhancing Wnt/β-catenin signaling activity promotes CPC proliferation while inhibiting their differentiation toward cardiomyocytes [12]. Therefore, we further investigate whether overexpression of the Wnt signaling pathway can rescue the hypoplastic OFT and RV phenotype observed in N-cadherin mutants.

First and foremost, we confirmed the presence of canonical Wnt/β-catenin signaling activity in AHF-CPCs with a BAT-GAL reporter mouse line, where lacZ gene is expressed under the control of β-catenin/TCF responsive elements [12]. Analysis of the X-gal-stained embryos at E9.5 indicated the presence of an active canonical Wnt/β-catenin signaling pathway in the AHF progenitor cells (Figure 4A).

Next, we investigated the relationship between N-cadherin and Wnt signaling in both mutant and wild-type AHF-CPCs. Using genetically altered mouse ES cell lines (Mutant: *AHF-Cre*; *AHF-GFP*; *Cdh2*$^{fl/fl}$ and wild

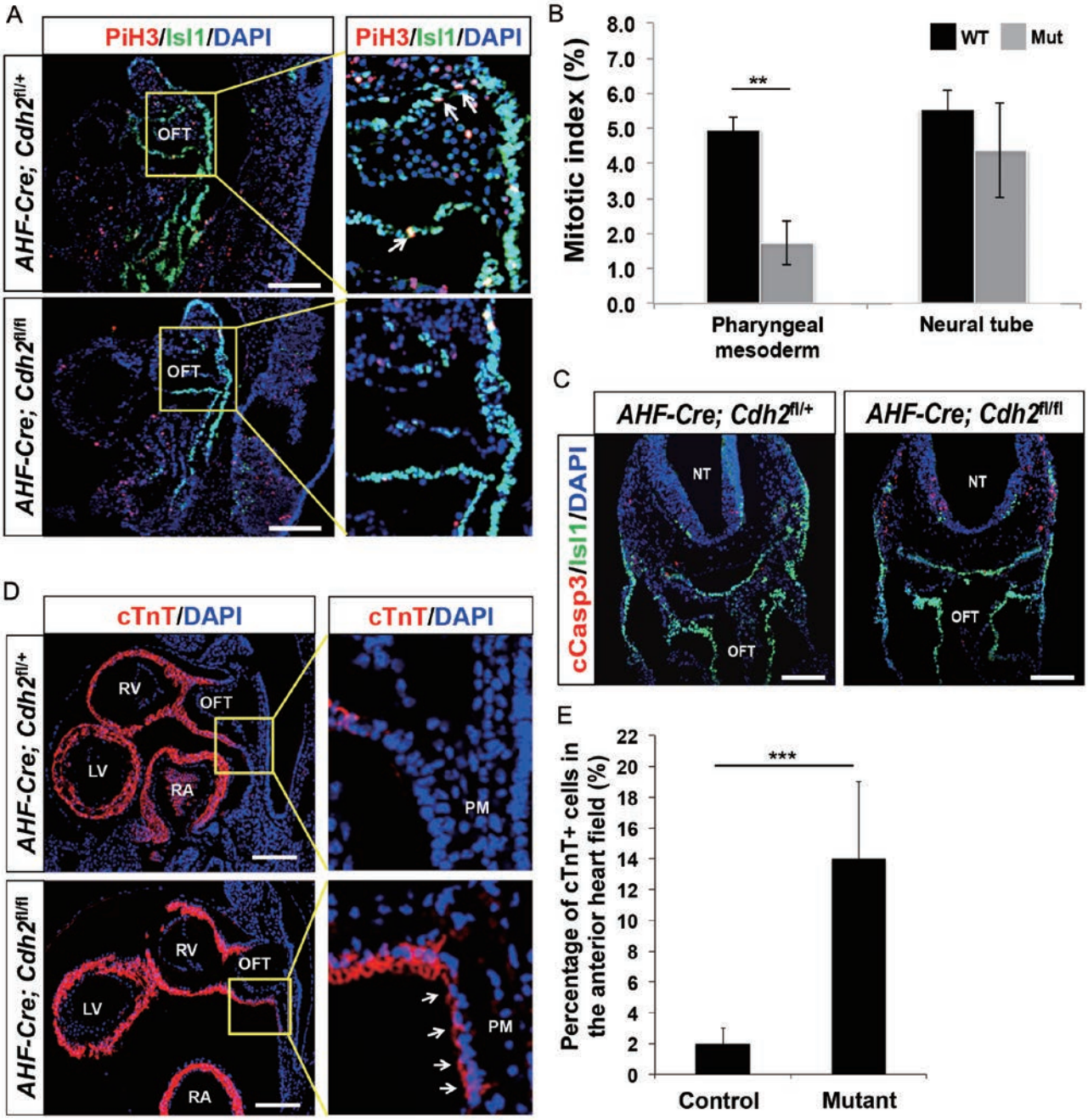

Figure 3 Loss of N-cadherin impairs proliferation and induces premature differentiation of AHF progenitor cells. **(A)** Representative sagittal section of control and mutant embryos at E9.5 immunostained for Isl1 (green) and phospho-Histone 3 (red); arrows point to Isl1/PiH3 double-positive cells in the OFT and AHF (enlarged image). Nuclei are marked by DAPI. Scale bar, 200 μm. **(B)** Quantification of cell proliferation indicated by mitotic index in the anterior heart field and neural tube regions of wild-type and mutants at E9.5. Error bars indicate SD, n = 4 experiments, $^{**}P$ = 0.01, evaluated by Student's t-test. **(C)** Representative transverse sections of control and mutant embryos at E9.0 immunostained for Isl1 (green) and cleaved Caspase 3 (red) in outflow tract (OFT) and neural tube (NT). Nuclei are marked by DAPI. Scale bar, 200 μm. **(D)** Sagittal sections of control and mutant embryos at E9.0 immunostained for cardiac troponin T (cTnT) (red). Note the presence of ectopic cTnT+ cells (arrows) in the AHF. Nuclei are marked by DAPI. Scale bar, 200 μm. **(E)** Quantification of cTnT+ cells in the AHF of the control and mutant embryos at E9.0. cTnT+ cells within the AHF, the region between OFT and anterior portion of pharyngeal mesoderm were counted. A total of 7-9 serial sections for each embryo were used. Error bars indicate SD, n = 6 embryos. $^{***}P$ = 0.001, evaluated by Student's t-test.

type: *AHF-Cre*; *AHF-GFP*; *Cdh2*$^{fl/+}$), GFP+ AHF-CPCs were sorted and re-plated for staining of either membrane-bound β-catenin or nuclear-bound β-catenin molecules. Notably, AHF-CPCs sorted from wild-type cells adhered significantly better than the cells isolated from *Cdh2* mutant (~15%; *P*-value = 0.0189) (Supplementary information, Figure S2). Employing high-content imaging to quantitate the intensities of β-catenin staining, a lower level of β-catenin was found to be present at the membrane of the N-cadherin mutant (Figure 4B). Interestingly, a lower level of β-catenin was also observed in the nuclei, suggesting an overall low level of β-catenin in the mutant AHF-CPCs as compared to the wild type (Figure 4B). These results were further validated by quantitative PCR of the sorted cells, whereby the Wnt molecules, Wnt signaling receptors, and, more importantly, Wnt signaling effectors (Axin2 and Lef1) were observed to be downregulated in the mutant CPCs (Figure

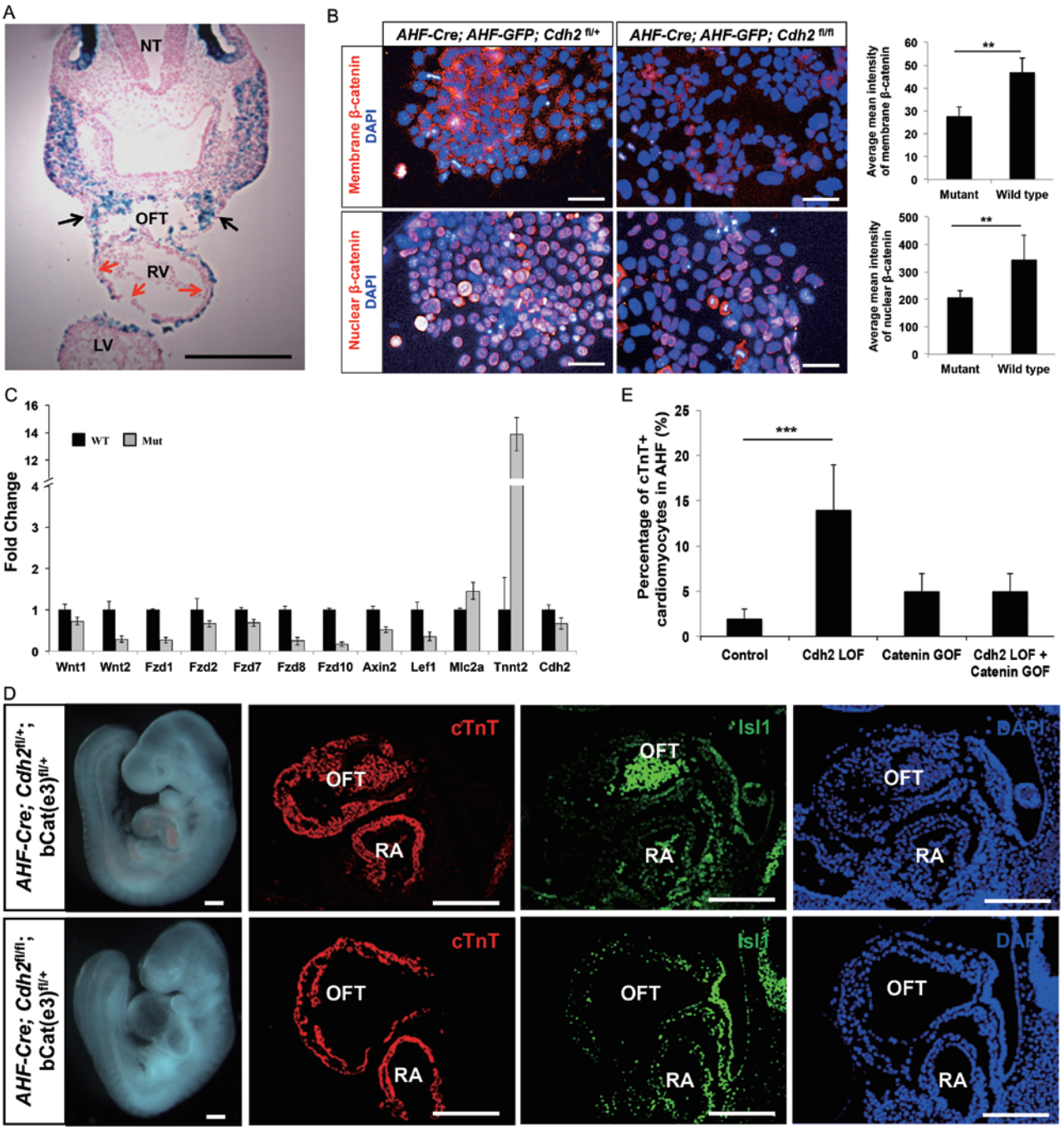

4C).

To assess the possibility of rescuing the N-cadherin mutant mice via overexpression of Wnt/β-catenin signaling, we introduced stabilized β-catenin in N-cadherin-deficient AHF-CPCs with a conditional mouse line for stabilized β-catenin ($Catnb^{+/lox(ex3)}$), where exon 3 of the β-catenin is flanked by loxP sites [12]. The protein fragment encoded by exon 3 contains the GSK target sites (serine and threonine), whose phosphorylation eventually leads to the degradation of β-catenin. Removal of exon 3 allows the protein to escape phosphorylation, thereby stabilizing it. Stabilization of β-catenin in regular CPCs and their progeny resulted in the dilation of the cardiac OFT and RV, as reported previously [12] (Figure 4D). Similarly, stabilization of β-catenin in N-cadherin-deficient CPCs and their progeny also resulted in the dilation of the cardiac OFT and RV when compared to *AHF-Cre*$^{+/-}$; *Cdh2*$^{fl/fl}$ mutants (Figure 4D, bottom panel and Figure 2B), although still smaller than β-catenin overexpression mutant. The analysis of AHF-CPCs in β-catenin/N-cadherin double mutants revealed that ectopic differentiation of CPCs into cTnT+ cells was downregulated in AHF (Figure 4E). In addition, the percentage of Isl1/PiH3 dual-positive cells in the AHF also increased in double mutants when compared to *AHF-Cre*; *Cdh2*$^{fl/fl}$ mutants (Supplementary information, Figure S3). Taken together, these results demonstrate that stabilization of β-catenin to a certain extent negates the effects of N-cadherin deficiency in AHF-CPCs.

Discussion

Previous studies have shown that global N-cadherin mutant embryos contain dramatic cell adhesion defects in the primitive heart where cardiomyocyte dissociation occurs even though myocardial tissue forms initially, thus resulting in eventual failure of the heart tube to form normally [18]. Deletion of N-cadherin in the *Mesp1-Cre* lineage also resulted in a more severe heart phenotype than in the *AHF-Cre* lineage. In *Mesp1-Cre* mutants, the entire heart tube is malformed and failed to loop, resulting in the hypoplastic development of both ventricles (Supplementary information, Figure S4). In this study, we document additional critical roles for N-cadherin at early stages of AHF progenitor formation, as the conditional deletion of N-cadherin in the *AHF-Cre* lineage leads to severe cardiac-specific phenotype that corresponds to dysfunction of the targeted AHF progenitor cell population. Phenotypes such as hypoplastic PM, OFT and RV in *AHF-Cre*$^{+/-}$; *Cdh2*$^{fl/fl}$ mutants indicate that N-cadherin is required for the regulation of proliferation and differentiation of Isl1+ AHF progenitors. The severity of the cardiac phenotype in the conditional N-cadherin knockout mutants in the current study suggests that N-cadherin is a critical cell adhesion molecule in establishing and maintaining early steps of heart progenitor cell fate and/or function. Because N-cadherin has been previously shown to play a key role in the assembly and maintenance of gap junctions in the myocardium [19], it is possible that the cardiac defect observed in the AHF conditional Cdh2 knockout mutant embryos is due to apoptosis of the AHF progenitors or the malfunction of the AHF-derived structures, in so causing the growth retardation and early embryonic lethality. Although an increase in apoptosis was observed in *AHF-Cre*$^{+/-}$; *Cdh2*$^{fl/fl}$ mutants compared to stage-controlled wild-type

Figure 4 Overexpression of Wnt signaling rescues *Cdh2* mutant phenotype. **(A)** Representative traverse section showing Wnt signaling activity in AHF progenitors as revealed by TCL/LEF-lacZ mice. Black arrows denote cells that have active Wnt signaling within pharyngeal mesoderm, whereas red arrows denote cells with inactive Wnt signaling within heart tube. Scale bar, 500 μm. **(B)** Representative images of AHF-CPCs isolated from wild type (*AHF-Cre*; *AHF-GFP*; *Cdh2*$^{fl/+}$) and mutant (*AHF-Cre*; *AHF-GFP*; *Cdh2*$^{fl/fl}$) stained red for either nuclear β-catenin or membrane-bound β-catenin. The average mean intensities were tabulated from 60 fields. Nuclei are marked by DAPI. A cut-off value >10 was imposed to remove background. Scale bar, 50 μm. Error bars indicate SD, n = 3 replicates, $^{**}P < 0.001$, evaluated by Student's t-test. **(C)** Quantitative PCR analysis of mRNA isolated from sorted progenitor cells (AHF-GFP+ CPCs) carrying AHF-GFP reporter transgene. The expression levels show that Wnt signaling ligands, receptors and effector genes (*Axin2* and *Lef1*) were downregulated in *Cdh2*-deficient progenitor cells, while upregulation of differentiation genes such as *Mlc2a* and *Tnnt2* were observed. Samples were normalized against the housekeeping gene, β-actin. Error bars indicate SD, n = 3 replicates. **(D)** Representative sagittal sections of single (*AHF-Cre*; *Cdh2*$^{fl/+}$; *bCat(e3)*$^{fl/+}$) and double (*AHF*-Cre; *Cdh2*$^{fl/fl}$; *bCat(e3)*$^{fl/+}$) mutants at E9.5. Sections stained for cTnT (red) and Isl1 (green) revealed similar expression patterns. Premature differentiation of Isl1+ CPCs into cTnT+ cells at the pharyngeal mesoderm was not observed in the double mutant as compared to single N-cadherin mutant (*AHF-Cre*; *Cdh2*$^{fl/fl}$) (Figure 3D). Nuclei are marked by DAPI. Scale bar, 100 μm. **(E)** Graphical representation of the number of cardiomyocytes (cTnT+ cells) in the AHF in various mutants (*AHF-Cre*; *Cdh2*$^{fl/fl}$, *AHF-Cre*; *Cdh2*$^{fl/+}$; *bCat(e3)*$^{fl/+}$ and *AHF-Cre*; *Cdh2*$^{fl/fl}$; *bCat(e3)*$^{fl/+}$) compared to control at E9.5 (somite number = 23-29). GOF, gain of function; LOF, loss of function. cTnT+ cells within the AHF, the region between OFT and the anterior portion of pharyngeal mesoderm, were counted. A total of 7-9 serial sections for each embryo were used. Error bars indicate SD, n = 6 embryos. $^{***}P$ = 0.001, evaluated by Student's t-test.

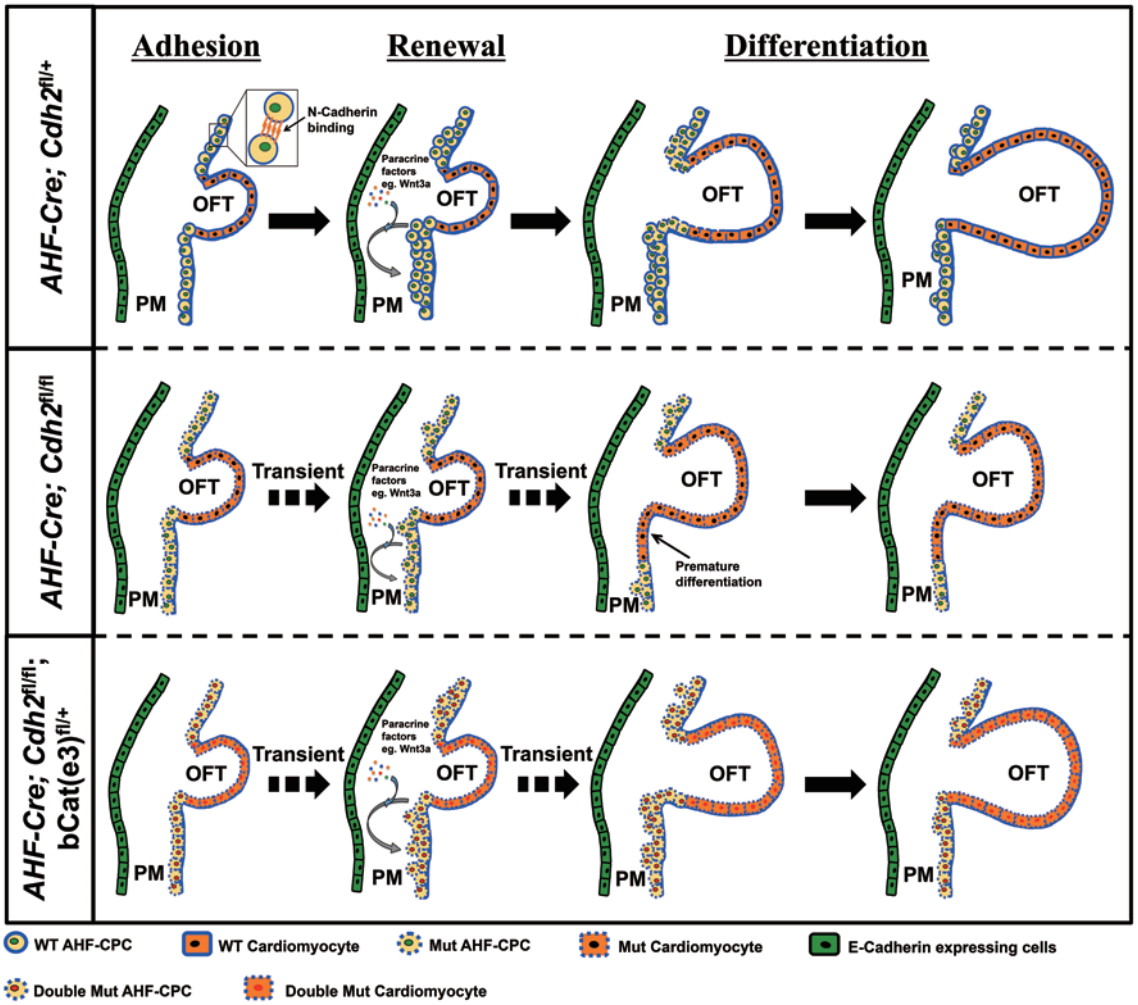

Figure 5 Schematic summarizing the role of N-cadherin in the maintenance of AHF-CPCs. In wild-type mice, N-cadherin expression by CPCs allows the cells to be properly adhered in the microenvironment of the pharyngeal mesoderm, thereby allowing the cells to be sufficiently exposed to paracrine factors that promote multipotency and proliferation. In addition, N-cadherin serves to maintain β-catenin levels by sequestering the molecules at the cell membrane. These allow the AHF-CPCs from wild-type mice to achieve higher Wnt signaling activity as compared to single mutant (*AHF-Cre*;*Cdh2*$^{fl/fl}$), where an overall downregulation of Wnt signaling activity was observed, which consequently resulted in premature differentiation of CPCs to cardiomyocytes in the AHF. Expectedly, activating Wnt signaling by overexpression of β-catenin in the double mutant (*AHF-Cre*; *Cdh2*$^{fl/fl}$; *bCat(e3)*$^{fl/+}$) was able to partially rescue the premature differentiation phenotype of the CPCs observed in *Cdh2* single mutant.

littermates, the increase occurred mostly in non-cardiac tissues such as the first branchial arch and neural tube (NT). Surprisingly, a small number of apoptotic cells was detected at the IFT of the heart, but not in the PM or at the distal part of OFT. We speculate that this localized cell death within the venous pole could be due to lack of survival signals mediated by cell-cell contact through N-cadherin. Indeed, previous studies showed that cell adhesion-mediated contacts by N-cadherin are required for expansion and survival of smooth muscle cells in the heart [24, 25]. The absence of apoptotic cells in the PM and distal portion of OFT of *Cdh2* mutant, however, could be due to the presence of the paracrine factors and/or signaling pathways that promote progenitor cell survival in an N-cadherin-independent manner. In contrast, deletion of N-cadherin reduces proliferation in the PM region and not in tissues unrelated to the AHF lineage, such as the NT. This decrease in proliferation of AHF progenitor accounts for the hypoplastic AHF-derived structures observed in the N-cadherin mutants.

In addition, several studies have previously reported that a high concentration of cadherin molecules can form

adherens junctions with β-catenin and sequester the latter at the cell membrane, thereby limiting its availability to function in the Wnt signaling pathway [12, 26, 27].

In our study, while Wnt signaling is highly active and positively regulates the AHF-CPCs in developing hearts of wild-type mice, the pathway is downregulated in *Cdh2* mutant. Examination of AHF-CPCs obtained from both wild-type and *Cdh2* mutants revealed that the latter had an overall downregulated Wnt signaling activity as a result of decreased expressions of Wnt signaling ligands and receptors (Figure 4C). Taken together, this suggests a possible upstream role of N-cadherin in the regulation of Wnt signaling in AHF-CPCs. In wild-type AHF-CPCs, N-cadherin sequesters β-catenin at the cell membrane, and prevents it from proteolytic degradation by the destruction complex. Upon Wnt ligand binding, β-catenin translocates into the nucleus, where it activates downstream gene targets. This mechanism allows the cell to maintain a certain threshold level of Wnt signaling, which has been shown to be important in the maintenance of CPCs [12]. However, such mechanism is absent in the *Cdh2* mutant. An overall low level of β-catenin within the CPCs causes the cells to lose their ability to self-renew, as indicated by a decreased mitotic index in the PM of the mutant (Figure 3B). A low level of β-catenin also accounts for occurrence of premature differentiation of CPCs to cardiomyocytes within the PM. Hence, it appears that a potential role of N-cadherin in the AHF-CPCs is to maintain β-catenin levels in the cytoplasm, which otherwise would be degraded by the β-catenin destruction complex as observed in the mutant.

Since N-cadherin plays a crucial role in cell adhesion and Wnt signaling of AHF-CPCs, a working model is suggested whereby the deletion of the adhesion molecule would inevitably perturb the physical cell adhesion system, proliferation and subsequent differentiation processes that are necessary for the formation of a highly organized organ such as the heart (Figure 5). As one of the early events in cardiogenesis involves the expansion of CPCs in the PM (niche), proper adhesion of the CPCs within the PM would allow the progenitor cells to be sufficiently exposed to paracrine factors that promote multipotency and proliferation [12]. This in turn results in a larger pool of CPCs in the PM, which is critical for proper cardiac development.

In N-cadherin mutants, the lack of cell adhesion molecules in the microenvironment of CPCs resulted in the progenitors to be loosely bound in their microenvironment. Coupled with an overall downregulation of Wnt signaling in the mutant CPCs, premature differentiation to cardiomyocytes occurs. Collectively, this resulted in a smaller pool of progenitor cells being available for proper cardiogenesis to occur. This explains for the observed phenotype in which the deletion of N-cadherin in the AHF lineage causes a dysregulation of AHF progenitor cells in the PM because not only do *AHF-Cre*$^{+/-}$; *Cdh2*$^{fl/fl}$ mutant embryos carrying the reporter *ROSA26-LacZ*$^{fl/+}$ (data not shown) have smaller PM regions that lack cellularity and structure compared to wild-type embryos, but their hypoplastic OFT and RV phenotypes, as a result of premature differentiation of CPCs to cardiomycytes, are also indicative of a dysregulation in AHF progenitor cell survival, proliferation, and differentiation.

Consistent with previous studies where the importance of Wnt signaling in the AHF during cardiogenesis was demonstrated [11], and through the maintenance of undifferentiated Isl1+ AHF progenitor cells *in vitro* with Wnt-overexpressing feeder layer [12], hypoplastic OFT and RV phenotypes observed in *Cdh2* mutants can be rescued by promoting proliferation of the AHF-CPCs through overexpression of the Wnt/β-catenin signaling pathway as depicted in the double mutant (*AHF-Cre*; *Cdh2*$^{fl/fl}$; *bCat(e3)*$^{fl/+}$). These results suggest a functional interaction between N-cadherin and canonical Wnt signals, whereby the adhesion of the AHF progenitors allows continued, prolonged exposure to Wnt signals, allowing their expansion in the absence of differentiation as suggested by our previous studies [12].

In conclusion, through *in silico* data analysis and genetic loss/gain of functions, we have shown in this study that N-cadherin plays an integral role during early cardiogenesis by maintaining high Wnt signaling activity in AHF-CPCs. Besides promoting proper adhesion of the CPCs within the AHF, high expression levels of Wnt signaling receptors were observed in wild-type CPCs, thereby allowing efficient response to paracrine signaling in the PM, which in turn promotes proliferation and prevents premature differentiation of the CPCs.

Materials and Methods

Mouse lines and genotyping

All animals were maintained in a pathogen-free environment. *AHF-Cre* mice were generously provided by Dr Brian Black (UCSF, CA) and described by Verzi *et al*. [22], where Cre recombinase expression is controlled by an enhancer/promoter region that exclusively directs expression to the AHF and its derivatives. Floxed Cdh2 mice were purchased from the Jackson Laboratory originally donated by Dr Glenn Radice (Jefferson Medical College, PA). Both *ROSA26-LacZ*$^{fl/+}$ and *ROSA26-GFP*$^{fl/+}$ were purchased from the Jackson Laboratory, while AHF-GFP knockin mice were generated in our lab. Homozygous floxed Cdh2 mice were crossed with AHF-Cre mice to generate doubly heterozygous *AHF-Cre*$^{+/-}$; *Cdh2*$^{fl/+}$ mice. These mice were then backcrossed to homozygous floxed Cdh2 mice to produce *AHF-Cre*$^{+/-}$; *Cdh2*$^{fl/+}$ mice, which served as wild-type littermate controls, and *AHF-Cre*$^{+/-}$; *Cdh-*

$2^{fl/fl}$, which are mutants null for the Cdh2 allele. A mouse strain in which exon 3 of β-catenin is flanked by loxP sites was generated previously by Harada *et al.* [28] (*Catnb*$^{+/lox(ex3)}$) and was obtained from Jackson Lab.

Progenies of the matings were genotyped using the following primer sets under PCR protocols described in their original publications. DNA was extracted from ear tags, tail tips and embryonic yolk sacs with 50 μl of Extraction Solution, 12 μl of Tissue Prep Solution, and 50 μl of Neutralization Solution B (Sigma E7526, T3073, and N3910).

Ahf-Cre: (Fwd) 5′-TGCCACGACCAAGTGACAGC-3′, (Rev) 5′-CCAGGTTACGGATATAGTTCATG-3′ (710 bp)

Cdh2 Floxed: (Fwd) 5′-CCAAAGCTGAGTGTGACTTG-3′, (Rev) 5′-TACAAGTTTGGGTGACAAGC-3′ (WT = 250 bp, MUT = 290 bp)

Embryo dissections and tissue isolation

In timed pregnancies, the day of a vaginal plug was considered embryonic day 0.5 (E0.5). Uteri containing embryos were dissected from females at various stages of pregnancy (E8.5-E12.5) and placed in cold PBS. Embryos were dissected from the uterus in their yolk sacs in dissection medium (2% FBS in PBS). The yolk sac and amnion were subsequently removed from the embryo and collected for genotyping. The embryos were fixed overnight with 4% PFA at 4 °C. Microdissection of the embryo was performed by further dissecting the heart tube from the embryo proper by incisions at the distal outflow and IFTs. The PM region was then removed by making an incision at the outflow and IFTs to the dorsal aorta and a longitudinal incision along the embryonic pharynx.

RNA isolation and quantitative PCR

Microdissected tissues prepared for RNA were flash frozen or stored in RNAlater RNA Stabilization Reagent (Qiagen 76104) until total RNA extraction using the RNeasy Mini Kit (Qiagen) with on-column DNaseI digestion. Briefly, RNA samples (100 ng) were reverse transcribed to obtain cDNA using the iScript cDNA Synthesis kit (BioRad). Primer sequences and PCR conditions are available upon request. Quantitative PCR (qPCR) analyses were performed using SYBR Green Master Mix Reagent (Applied Biosystems) on an ABI Viia7 Real Time PCR System. Standard deviations (SD) of the means in qPCR experiments were obtained from three independent experiments.

Cryosection and immunohistochemistry

Embryos fixed overnight in 4% PFA were washed extensively with PBS without Ca^{2+} and Mg^{2+} and transferred to 15% sucrose in PBS without Ca^{2+} and Mg^{2+} (W/V) for overnight saturation at 4 °C. Embryos were then transferred to 30% sucrose in PBS (W/V) for 30 min followed by a series of four 5-min incubations in OCT Cryosection Compound (Sakura Finetec 4583) until equilibration. Processed embryos were transferred to cryosection blocks in OCT compound and adjusted until the desired orientation was achieved. Once set, the block was lowered into a dry-ice/ethanol bath to freeze the OCT. Mounted embryos in OCT were stored at −80 °C and thawed at −20 °C before cryosection. Embryos in OCT blocks were trimmed, mounted onto cryosection chucks and sectioned at −19 °C operating temperature and −21 °C cutting temperature. The sections were 8 μm thick and were placed onto Superfrost Plus slides (Fisher Scientific 12-550-15) in a serial manner. Finished slides were stored at −80 °C.

Immunohistochemistry was performed on the sections by first washing the cryosection slides in PBS without Ca^{2+} and Mg^{2+} for 5 min at RT to remove the OCT and then washed in PBS with 0.1% saponin (Sigma 47036) for another 10 min at RT to permeabilize the cells. The sections were placed in blocking solution (10% horse serum and 2% bovine serum albumin in 0.1% saponin PBS solution) for 1 h at 37 °C and then incubated with primary antibody diluted in blocking solution overnight at 4 °C. Sections were washed three times for 5 min each in blocking solution at RT and incubated with the respective secondary antibodies diluted in blocking solution for 1 h at 37 °C. The sections were then washed four times for 5 min each in PBS with 0.1% saponin and mounted with a cover slip using Fluorescence Mounting Medium (Dako S3023). The primary antibodies used were rabbit anti-N-cadherin (1:100; Millipore 1126), mouse anti-Isl1 (1:200; Hybrodoma Bank 39.4D5), mouse anti-PY654-β-catenin (membrane bound) (Hybridoma bank), mouse anti-PY489-β-catenin (nuclear) (Hybridoma bank), rat anti-E-cadherin (1:100; Santa Cruz sc-59778) and mouse anti-cardiac troponin T (1:400; Abcam ab8295). The secondary antibodies included Alexa fluor 488-conjugated goat anti-mouse (1:500; Molecular Probes A11001), Alexa fluor 594-conjugated goat anti-rat (1:500; Molecular Probes A11007) and Alexa fluor 594-conjugated goat anti-rabbit (1:500; Molecular Probes A11012). DAPI nuclei stain (1:1 000); Molecular Probes (D1306) was added directly to the blocking solution with the secondary antibodies.

Paraffin section and H&E staining

Embryos fixed overnight in 4% PFA were washed extensively with PBS without Ca^{2+} and Mg^{2+} and dehydrated through a progressively more concentrated ethanol series (50%, 70%, 90% and 100%; 2 washes each for 30 min). The embryos were then transferred to a 50:50 mixture of ethanol and xylene for 1 h, pure xylene for 1 h and a 50:50 mixture of xylene and paraffin overnight at 58 °C. The embryos were then transferred to a pure paraffin solution at 58 °C and incubated for 3 h before embedding into preheated plastic molds in either a sagittal or transverse orientation. Embedded embryos were cooled to allow the paraffin to solidify. Paraffin sections were prepared at 8 μm and dried on a heating block at 37 °C overnight.

For H&E staining, the sections were deparaffinized by incubation in pure xylene and a 50:50 mixture of xylene and ethanol for 10 min each. The sections were then placed in 100% ethanol and rehydrated through a progressively decreasing ethanol series (90%, 70% and 50%; 2 washes each for 5 min each) until washed with distilled water for 2 min. The sections were then stained in Harris hematoxylin solution (Sigma) for 5 min at RT and washed in running distilled water for 3 min followed by differentiation in 1% acid alcohol for 30 s. After rinsing in running tap water for 3 min, the sections were dipped 6 times in 0.1% ammonia water (V/V) and rinsed again under running tap water for 3 min at RT. Finally, the sections were stained in Eosin Y solution (Sigma), washed under running tap water for 3 min and dehydrated through an ethanol series to pure xylene and mounted with a cover slip using Permount Mounting Medium (Fisher Scientific SP15-500).

LacZ staining

The *ROSA26-LacZ*$^{fl/+}$ reporter was crossed into the Cdh2 floxed

background and mated with *AHF-Cre*$^{+/-}$; *Cdh2*$^{fl/+}$ males to generate litters of wild-type and conditional Cdh2 knockout mutant embryos that were also LacZ-positive for regions that express Cre-recombinase. After fixation in 4% PFA in PBS for 20 min at RT, the embryos were rinsed in PBS and washed 3 times in wash buffer (2 mM $MgCl_2$, 0.01% deoxycholate, 0.02% NP40 in 0.1 M sodium phosphate pH 7.3) at RT for 30 min each. X-Gal staining solution (1 mg/mL X-gal, 4 mM potassium ferrocyanide, 4 mM potassium ferricyanide, 20 mM Tris pH 7.3 in wash buffer) was added to the embryos and kept at RT in the dark until the desired level of staining was achieved. The stain was poured off and the embryos were washed 2 times in wash buffer at RT for 1 h each followed by fixation in 4% PFA for 1 h to prevent background LacZ signal development. The stained embryos were stored in 70% glycerol at 4 °C for further analysis.

Cell death and proliferation assays

Wild-type littermate control and mutant embryos were collected at various stages and fixed overnight with 4% PFA. 8 μm transverse or sagittal sections were produced as described above and stained with rabbit anti-phospho-histone 3 (1:1 000; Upstate) as a marker of cell proliferation and with rabbit anti-cleaved caspase 3 (1:200; Millipore) as a marker of cell death. Alexa fluor 594-conjugated goat anti-rabbit (1:500; Molecular Probes) was used as secondary antibody. Each section was also co-stained for Isl1 to demarcate the PM region and distinguish AHF progenitor cells from other populations.

Representative IHC images from multiple wild-type littermate control and mutant embryos with matching sections were used for the cell death and proliferation analysis. While cell death analysis was performed on an observational basis, cell proliferation was quantified by a mitotic index, described as the percentage of phospho-histone 3-positive cells compared to the total number of Isl1+ cells in the PM. The NT mitotic index was calculated as the percentage of phospho-histone 3-positive cells compared to the total number of DAPI+ cells in the NT. Cells were counted both manually with a click-counter and automatically by the ImageJ Particle Analysis tool, independently in a randomized blind manner to reduce biases in the results and to provide independent data verification. Four wild type-mutant pairs were counted, each with four sections, in both the PM region and also the NT region as a control region not directly affected by the conditional deletion of Cdh2 by AHF-Cre. The collected data was analyzed for mean, standard deviation and standard error. An unpaired two-tailed Student's *t*-test was performed to determine the significance of the difference in mitotic index observed between the wild-type and mutant embryos ($P < 0.05$ is highly significant). Data are reported as mean ± SEM.

Image analysis of nuclear and cytoplasmic β-catenin

Using genetically altered mouse ES cell lines (Mutant: *AHF-Cre*; *AHF-GFP*; *Cdh2*$^{fl/fl}$ and wild type: *AHF-Cre*; *AHF-GFP*; *Cdh2*$^{fl/+}$), GFP+ AHF-CPCs were sorted and seeded at 30 000 cells per well of a 96-well plate. The cells were allowed to adhere overnight. Thereafter, they were fixed, and stained with either a nuclear β-catenin antibody (PY489 β-catenin) or a cytoplasmic β-catenin antibody (PY654 β-catenin) at 1:500 dilutions, and nuclei were counterstained with DAPI (both antibodies from Hybridoma Bank). Images were acquired by an automated microscope (PerkinElmer Operetta) at 20× magnification. Image analysis was performed on 3 biological replicates (60 fields each) using the Columbus software (PerkinElmer).

Statistics

qPCR values are expressed as mean ± SD. Results were tested for statistical significance using Student's *t*-test, two sided based on assumed normal distributions. $P < 0.05$ were considered statistically significant.

Acknowledgments

This work was supported in part by the Research Grant Council of HKSAR (T13-706/11).

References

1 Buckingham M, Meilhac S, Zaffran S. Building the mammalian heart from two sources of myocardial cells. *Nature Rev Genet* 2005; **6**:826-835.
2 Laugwitz KL, Moretti A, Caron L, Nakano A, Chien KR. Islet1 cardiovascular progenitors: a single source for heart lineages? *Development* 2008; **135**:193-205.
3 Martin-Puig S, Wang Z, Chien KR. Lives of a heart cell: tracing the origins of cardiac progenitors. *Cell Stem Cell* 2008; **2**:320-331.
4 Yang L, Cai CL, Lin L, *et al*. Isl1Cre reveals a common Bmp pathway in heart and limb development. *Development* 2006; **133**:1575-1585.
5 Kelly RG, Brown NA, Buckingham ME. The arterial pole of the mouse heart forms from Fgf10-expressing cells in pharyngeal mesoderm. *Dev Cell* 2001; **1**:435-440.
6 Ilagan R, Abu-Issa R, Brown D, *et al*. Fgf8 is *required* for anterior heart field development. *Development* 2006; **133**:2435-2445.
7 Park EJ, Watanabe Y, Smyth G, *et al*. An FGF autocrine loop initiated in second heart field mesoderm regulates morphogenesis at the arterial pole of the heart. *Development* 2008; **135**:3599-3610.
8 Goddeeris MM, Schwartz R, Klingensmith J, Meyers EN. Independent requirements for Hedgehog signaling by both the anterior heart field and neural crest cells for outflow tract development. *Development* 2007; **134**: 1593-1604.
9 Rochais F, Mesbah K, Kelly RG. Signaling pathways controlling second heart field development. *Circ Res* 2009; **104**:933-942.
10 Reya T, Clevers H. Wnt signalling in stem cells and cancer. *Nature* 2005; **434**:843-850.
11 Kwon C, Arnold J, Hsiao EC, Taketo MM, Conklin BR, Srivastava D. Canonical Wnt signaling is a positive regulator of mammalian cardiac progenitors. *Proc Natl Acad Sci USA* 2007; **104**: 10894-10899.
12 Qyang Y, Martin-Puig S, Chiravuri M, *et al*. The renewal and differentiation of Isl1+ cardiovascular progenitors are controlled by a Wnt/beta-catenin pathway. *Cell Stem Cell* 2007; **1**:165-179.
13 Fuller MT, Spradling AC. Male and female *Drosophila* germline stem cells: two versions of immortality. *Science* 2007; **316**:402-404.
14 Zhang J, Niu C, Ye L, *et al*. Identification of the haemato-

poietic stem cell niche and control of the niche size. *Nature* 2003; **425**:836-841.
15 Fuchs E, Tumbar T, Guasch G. Socializing with the neighbors: stem cells and their niche. *Cell* 2004;**116**:769-778.
16 Linask KK. N-cadherin localization in early heart development and polar expression of Na+,K(+)-ATPase, and integrin during pericardial coelom formation and epithelialization of the differentiating myocardium. *Dev Biol* 1992; **151**:213-224.
17 Linask KK, Knudsen KA, Gui YH. N-cadherin-catenin interaction: necessary component of cardiac cell compartmentalization during early vertebrate heart development. *Dev Biol* 1997; **185**:148-164.
18 Radice GL, Rayburn H, Matsunami H, Knudsen KA, Takeichi M, Hynes RO. Developmental defects in mouse embryos lacking N-cadherin. *Dev Biol* 1997; **181**:64-78.
19 Li J, Patel VV, Kostetskii I, *et al*. Cardiac-specific loss of N-cadherin leads to alteration in connexins with conduction slowing and arrhythmogenesis. *Circ Res* 2005; **97**:474-481.
20 Domian IJ, Chiravuri M, van der Meer P, *et al*. Generation of functional ventricular heart muscle from mouse ventricular progenitor cells. *Science* 2009; **326**:426-429.
21 Vincent SD, Buckingham ME. How to make a heart: the origin and regulation of cardiac progenitor cells. *Curr Top Dev Biol* 2010; **90**:1-41.
22 Verzi MP, McCulley DJ, De Val S, Dodou E, Black BL. The right ventricle, outflow tract, and ventricular septum comprise a restricted expression domain within the secondary/anterior heart field. *Dev Biol* 2005; **287**:134-145.
23 Kostetskii I, Li J, Xiong Y, *et al*. Induced deletion of the N-cadherin gene in the heart leads to dissolution of the intercalated disc structure. *Circ Res* 2005; **96**:346-354.
24 Uglow EB, Slater S, Sala-Newby GB, *et al*. Dismantling of cadherin-mediated cell-cell contacts modulates smooth muscle cell proliferation. *Circ Res* 2003; **92**:1314-1321.
25 Koutsouki E, Beeching CA, Slater SC, Blaschuk OW, Sala-Newby GB, George SJ. N-cadherin-dependent cell-cell contacts promote human saphenous vein smooth muscle cell survival. *Arterioscl Thromb Vasc Biol* 2005; **25**:982-988.
26 Kam Y, Quaranta V. Cadherin-bound beta-catenin feeds into the Wnt pathway upon adherens junctions dissociation: evidence for an intersection between beta-catenin pools. *PloS One* 2009; **4**:e4580.
27 Valenta T, Hausmann G, Basler K. The many faces and functions of beta-catenin. *EMBO J* 2012; **31**:2714-2736.
28 Harada N, Tamai Y, Ishikawa T, *et al*. Intestinal polyposis in mice with a dominant stable mutation of the beta-catenin gene. *EMBO J* 1999; **18**:5931-5942.

(**Supplementary information** is linked to the online version of the paper on the *Cell Research* website.)